

Estimation of neuronal responses from fMRI data

M. Havlicek, *Member, IEEE*, J. Jan, M. Brazdil, and V.D. Calhoun, *Senior Member, IEEE*

Abstract - In this paper we describe a deconvolution technique for estimation of the neuronal signal from an observed hemodynamic responses in fMRI data. Our approach, based on the Rauch-Tung-Striebel smoother for square-root cubature Kalman filter, enables us to accurately infer the hidden states, parameters, and the input of the dynamic system. Additionally, we enhance the cubature Kalman filter with a variational Bayesian approach for adaptive estimation of the measurement noise covariance.

I. INTRODUCTION

Observed functional magnetic resonance imaging (fMRI) the observed hemodynamic response is an indirect measure of neuronal activation, i.e. the response is represented by changes in blood flow and blood oxygenation that follow after neuronal activation. Moreover, this complex relationship can be both subject and brain region specific, which makes identification of the true effective connectivity (directional influence) between different brain regions difficult. Fortunately, the hemodynamic model describing this relation has been characterized [1], [2], which, under certain assumptions, allows an inversion of the hidden dynamic process to obtain an estimate of the neuronal activation given some observations.

The Bayesian framework is the most commonly used method for the study of dynamic systems that allows inference on the hidden states, model parameters and the input. However, since the hemodynamic balloon model possesses strong nonlinear characteristics, we need to use a nonlinear estimation procedure. Taking this into account, we propose a deconvolution technique based on the recently introduced cubature Kalman filter (CKF) [3], which is the closest known direct approximation to the Bayesian filter and has been shown to outperform all other nonlinear filters

Manuscript received March 26, 2011. This work has been sponsored by the research center DAR no. 1M0572, and also supported by the research frame no. MSM0021630513 and no. MSM0021622404, all funded by the Ministry of Education, Czech Republic. Next, there was a support from the Grand Agency of Czech Republic no. P304/11/1318. From the USA side, it has been funded by NIH grant no. R01EB000840.

M. Havlicek is with the Dept. of Biomedical Engineering, FEEC, Brno University of Technology, Czech Republic, and with the Mind Research Network, Albuquerque, NM, USA (e-mail: havlicekmartin@gmail.com).

J. Jan is with the Dept. of Biomedical Engineering, FEEC, Brno University of Technology, Czech Republic (email: jan@feec.vutbr.cz).

M. Brazdil is with the Dept. of Neurology, St. Anne's University Hospital, and Faculty of Medicine, Masaryk University, Brno, Czech Republic (e-mail: mbrazd@med.muni.cz).

V. D. Calhoun is with the Mind Research Network and the Dept. of ECE, University of New Mexico, Albuquerque, NM, USA (e-mail: vcalhoun@unm.edu).

in a Gaussian environment. Specifically, we apply CKF that is finessed by a backward pass of cubature Rauch-Tung-Striebel (RTS) smoother to simultaneously infer hidden states, parameters and estimate the input (neuronal synaptic activity). Additionally, we enhance CKF with variational Bayesian approach for adaptive estimation of the measurement noise covariance [9].

II. METHODS

A. Continuous-discrete dynamic models

Nonlinear filtering problems are typically described by state-space models comprising a process and measurement equation. In many practical problems, the process equation is derived from the underlying physics of a continuous dynamic system, and is expressed in the form of a set of differential equations. Since the measurements y are available at discrete times ($t = 1, 2, \dots, T$), we have a model with a continuous process equation and a discrete measurement equation in stochastic form:

$$\begin{aligned} dx_t &= \mathbf{h}(x_t, \theta_t, u_t, t)dt + \mathbf{I}(x_t, t)d\beta_t \\ y_t &= \mathbf{g}(x_t, \theta_t, t) + r_t, \end{aligned} \quad (1)$$

where θ_t represents unknown parameters of the equation of motion \mathbf{h} and the measurement function \mathbf{g} , respectively; u_t is the exogenous input that drives the hidden states; $r_t \sim \mathcal{N}(0, R_t)$ is a vector of Gaussian measurement noise; $\mathbf{I}(x_t, t)$ can be a function of the states and time; and β_t denotes a Wiener process or state noise that is assumed to be independent of states and measurement noise. The continuous time formulation of the stochastic differential equations (SDE) can be converted into a discrete-time analogue using e.g. local linearization (LL) scheme [4]:

$$\begin{aligned} x_t &= \mathbf{f}(x_{t-1}, \theta_{t-1}, u_{t-1}) + q_{t-1}, \\ y_t &= \mathbf{g}(x_t, \theta_t) + r_t, \end{aligned} \quad (2)$$

where q_t is a Gaussian state noise vector; $q_t \sim \mathcal{N}(0, Q_t)$. In this case, the function $\mathbf{f}(\cdot)$ is evaluated through:

$$\mathbf{f}(\cdot) \approx x_{t-1} + f_{x_t}^{-1}[\exp(f_{x_t} \Delta t) - I] \mathbf{h}(x_{t-1}, \theta_{t-1}, u_{t-1}). \quad (3)$$

Here f_{x_t} is a Jacobian of \mathbf{h} and Δt is the time interval between samples (up to the sampling interval). The LL-scheme has demonstrated to improve the convergence and stability properties of conventional numerical integrators [4]. See [5] for its simple algebraic representation.

B. Nonlinear model identification

Parameter estimation sometimes referred to as system identification can be regarded as a special case of general state estimation in which the parameters are absorbed into the state vector. Parameter estimation involves determining nonlinear mapping:

$$y_t = \mathcal{D}(x_t; \theta_t), \quad (4)$$

where the nonlinear map $\mathcal{D}(\cdot)$ is, in our case, the dynamic model $\mathbf{f}(\cdot)$ parameterized by the vector θ_t . The parameters θ_t correspond to a stationary process with identity state transition matrix, driven by an ‘‘artificial’’ process noise $w_t \sim \mathcal{N}(0, W_t)$. The input or cause of motion on hidden states u_t can be estimated as well, with input noise $v_t \sim \mathcal{N}(0, V_t)$. This is possible because of the so-called natural condition of control [3], which says that the input u_t can be generated using the state prediction $\hat{x}_{t|t-1}$. In the case, the ‘‘input’’ to the nonlinear mapping function $\mathcal{D}(\cdot)$, i.e. our hidden states x_t , cannot be observed, one can apply a joint filtering approach [6]. Here the unknown system states and parameters are concatenated into a single higher-dimensional joint state vector, $\mu = [x_t, u_t, \theta_t]^T$ and simultaneously estimated from the observed signal y_t . Then the state-space model has the form:

$$\mu_t = \begin{bmatrix} x_t \\ u_t \\ \theta_t \end{bmatrix} = \begin{bmatrix} \mathbf{f}(x_{t-1}, \theta_{t-1}, u_{t-1}) \\ u_{t-1} \\ \theta_{t-1} \end{bmatrix} + \begin{bmatrix} q_{t-1} \\ v_{t-1} \\ w_{t-1} \end{bmatrix} \quad (5)$$

$$y_t = \mathbf{g}(\mu_t) + r_{t-1}.$$

For simplicity, we will further denote the first bracket on the right side of the process equation by $\mathbf{F}(x_{t-1}, u_{t-1}, \theta_{t-1})$.

C. Cubature Kalman Filter

The cubature Kalman filter [3] is a recursive, nonlinear filtering algorithm. It computes the first two order moments (i.e. mean and covariance) of all conditional densities using a highly efficient numerical integration method (cubature rules). Specifically, it utilizes the third-degree spherical-radial rule to approximate the integrals of the form (*nonlinear function* \times *Gaussian density*) numerically using a set of m equally weighted symmetric cubature points $\{\xi_i, \omega_i\}_{i=1}^m$:

$$\int_{\mathbb{R}^n} \mathbf{f}(\mu) \mathcal{N}(\mu; 0, I_n) d\mu \approx \sum_{i=1}^m \omega_i \mathbf{f}(\xi_i), \quad (6)$$

$$\xi = \sqrt{\frac{m}{2}} [I_n, -I_n], \quad \omega_i = \frac{1}{m}, \quad i = 1, 2, \dots, m = 2n. \quad (7)$$

where ξ_i is the i -th column of cubature points matrix ξ with weights ω_i and n is dimension of the state vector ($n = n_x + n_u + n_\theta$).

In order to evaluate the dynamic state-space model described by (3), the CKF includes two steps: a) a time update, after which the predicted density $p(x_t | y_{1:t-1}) = \mathcal{N}(\hat{x}_{t|t-1}, P_{t|t-1})$ is computed; and b) a measurement update, after which the posterior density $p(x_t | y_{1:t}) = \mathcal{N}(\hat{x}_{t|t}, P_{t|t})$ is computed. Additionally, to improve

ALGORITHM I.

SQUARE-ROOT CUBATURE KALMAN FILTER WITH ESTIMATION OF MEASUREMENT NOISE COVARIANCE

• Initialization:

$$\hat{\mu}_0 = E[\mu_0] = [x_0, u_0, \theta_0]^T; \quad \lambda_0 = m - n_r; \quad {}^1B = \sqrt{\rho} I_{n_r}$$

$$S_0 = \text{diag}(\sqrt{P_{x_0}}, \sqrt{P_{u_0}}, \sqrt{P_{\theta_0}})$$

• Time update:

$$\mathcal{X}_{i,t-1|t-1} = S_{t-1|t-1} \xi_i + \hat{\mu}_{t-1|t-1}, \quad (8)$$

$$\mathcal{X}_{i,t|t-1}^* = \mathbf{F}(\mathcal{X}_{i,t-1|t-1}^x, \mathcal{X}_{i,t-1|t-1}^u, \mathcal{X}_{i,t-1|t-1}^\theta), \quad (9)$$

$$\hat{\mu}_{t|t-1} = \frac{1}{m} \sum_{i=1}^m \mathcal{X}_{i,t|t-1}^*, \quad (10)$$

$${}^2\sqrt{Q_t} = \text{diag}((1/\sqrt{\gamma} - 1)S_{t-1|t-1}^x), \quad (11)$$

$${}^3S_{t|t-1} = \text{qr}([X_{t|t-1}, \text{diag}(\sqrt{Q_t}, \sqrt{V_t}, \sqrt{W_t})]), \quad (12)$$

$$X_{t|t-1} = \frac{1}{\sqrt{m}} [\mathcal{X}_{1,t|t-1}^* - \hat{\mu}_{t|t-1}, \mathcal{X}_{2,t|t-1}^* - \hat{\mu}_{t|t-1}, \dots, \mathcal{X}_{m,t|t-1}^* - \hat{\mu}_{t|t-1}], \quad (13)$$

$$\lambda_{t|t-1} = \rho(\lambda_{t-1|t-1} - k - 1) + k + 1, \quad (14)$$

$$\Psi_{t|t-1} = B \Psi_{t-1|t-1} B^T \quad (15)$$

• Measurement update: Set $\hat{\mu}_{t|t-1}^{(0)} = \hat{\mu}_{t|t-1}$, $X_{t|t-1}^{(0)} = X_{t|t-1}$, $\Psi_{t|t-1}^{(0)} = \Psi_{t|t-1}$, and $\lambda_{t|t} = \lambda_{t|t-1} + 1$.

$$X_{t|t-1}, \Psi_{t|t-1}^{(0)} = \Psi_{t|t-1}, \text{ and } \lambda_{t|t} = \lambda_{t|t-1} + 1.$$

$$\mathcal{X}_{i,t|t-1} = S_{t|t-1} \xi_i + \hat{\mu}_{t|t-1} \quad (16)$$

$$\mathcal{Y}_{i,t|t-1} = \mathbf{g}(\mathcal{X}_{i,t|t-1}^x, \mathcal{X}_{i,t|t-1}^u, \mathcal{X}_{i,t|t-1}^\theta), \quad (17)$$

$$\hat{y}_{t|t-1} = \frac{1}{m} \sum_{i=1}^m \mathcal{Y}_{i,t|t-1}. \quad (18)$$

Iterate the following steps ($j = 1, \dots, J$):

$$S_{yy,t|t-1}^{(j+1)} = \text{qr}([Y_{t|t-1}, \sqrt{R_t}]), \quad (19)$$

$$R_t = (\lambda_{t|t} - k - 1)^{-1} \Psi_{t|t}^{(j)} \quad (21)$$

$$Y_{t|t-1} = \frac{1}{\sqrt{m}} [\mathcal{Y}_{1,t|t-1} - \hat{y}_{t|t-1}, \mathcal{Y}_{2,t|t-1} - \hat{y}_{t|t-1}, \dots, \mathcal{Y}_{m,t|t-1} - \hat{y}_{t|t-1}] \quad (22)$$

$$P_{\mu y,t|t-1} = X_{t|t-1}^{(0)} Y_{t|t-1}^T, \quad (23)$$

$$K_t^{(j+1)} = (P_{\mu y,t|t-1} / S_{yy,t|t-1}^{(j+1)T}) / S_{yy,t|t-1}^{(j+1)}, \quad (24)$$

$$\hat{\mu}_{t|t}^{(j+1)} = \hat{\mu}_{t|t-1}^{(0)} + K_t^{(j+1)} (y_t - \hat{y}_{t|t-1}), \quad (25)$$

$$S_{t|t}^{(j+1)} = \text{qr}([X_{t|t-1}^{(0)} - K_t^{(j+1)} Y_{t|t-1}, K_t^{(j+1)} \sqrt{R_t}]). \quad (26)$$

$$\mathcal{X}_{i,t|t} = S_{t|t}^{(j+1)} \xi_i + \hat{\mu}_{t|t}^{(j+1)}, \quad (27)$$

$$\mathcal{Y}_{i,t|t}^* = \mathbf{g}(\mathcal{X}_{i,t|t}^x, \mathcal{X}_{i,t|t}^u, \mathcal{X}_{i,t|t}^\theta), \quad (28)$$

$$\Psi_{t|t}^{(j+1)} = \Psi_{t|t-1}^{(0)} + D_t D_t^T, \quad (29)$$

$$D_t = \frac{1}{\sqrt{m}} [\mathcal{Y}_{1,t|t}^* - y_t, \mathcal{Y}_{2,t|t}^* - y_t, \dots, \mathcal{Y}_{m,t|t}^* - y_t] \quad (30)$$

If ($j = J$) set $\Psi_{t|t} = \Psi_{t|t}^{(J)}$, $\hat{\mu}_{t|t} = \hat{\mu}_{t|t}^{(J)}$, $S_{t|t} = S_{t|t}^{(J)}$, and

update W_t according to (31).

numerical stability of the filter, the square-root version of CKF (SCKF) is considered, where the square-root factors of the predictive and posterior error covariance matrices S are propagated ($P = SS^T$). For detail derivation of CKF see [3].

¹ Parameter $\rho \in (0, 1]$ defines assumed dynamics of the noise covariance ($\rho = 1$ corresponds to stationary covariance).

² Parameter $\gamma \in (0, 1]$ annealing rate and in our case $\gamma = 0.9995$.

³ Term $\text{qr}(\cdot)$ represents QR decomposition of matrix X^T into an orthogonal matrix Q and upper triangular matrix R such that $X^T = QR$, and $XX^T = R^T Q^T QR = R^T R = SS^T$, where the resulting square-root (lower triangular) matrix is $S = R^T$.

D. Adaptive estimation of noise covariance

In [9] a robust variational Bayesian (VB) approach for approximation of joint filtering distribution of the states and measurement covariance matrix was introduced, where the matrix R_t is modeled through the inverse Wishart (IW) distribution; $E[R_t] = (\lambda_t - k - 1)^{-1}\Psi_t$. Specifically, this involves dynamic models (14-15) for parameters λ_t and Ψ_t during the time update of CKF and their iterative update during the measurement update step (18-29). For a full and detail derivation of this VB approach see [9].

Besides measurement covariance matrix, we also approximate the noise covariance matrix W_t of model parameters by using a Robbins-Monro stochastic approximation scheme for estimating the innovations [6]:

$$W_t = (1 - \alpha)W_{t-1} + \alpha \tilde{K}_t (y_t - \hat{y}_{t|t-1})(y_t - \hat{y}_{t|t-1})^T \tilde{K}_t^T, \quad (31)$$

where \tilde{K}_t is the partition of Kalman gain matrix corresponding to the parameter variables, and $\alpha \in (0,1]$ is scaling parameter usually chosen to be a small number (e.g. 0.001). Moreover, we constrain W_t to be diagonal matrix, which implies an independence assumption on the parameters. Finally, we inject process noise artificially by annealing the square-root covariance of process noise (11).

The complete CKF algorithm with VB measurement noise covariance estimation is shown in Algorithm I.

E. Rauch-Tung-Striebel smoother

The following procedure is a backward pass of cubature RTS smoother, which can be used for computing suitable corrections to the forward filtering results to obtain the smoothing solution $p(x_t, y_{1:T}) = \mathcal{N}(\hat{x}_{t|T} | \hat{x}_{t|T}^S, P_{t|T}^S)$ [7]. Because the smoothing and filtering estimates of the last time step T are the same, we make $\hat{\mu}_{T|T}^S = \hat{\mu}_{T|T}$, $S_{T|T}^S = S_{T|T}$. This means the recursion can be used for computing the smoothing estimates of all time steps by starting from the last step $t = T$ and proceeding backwards to initial time step $t = 0$. The algorithm is summarized in Algorithm II.

Finally, in order to obtain optimal estimates of all parameters, states and input, we iterate over forward and backward run until the increase of the log-likelihood (32), calculated for each iteration, is less than a tolerance value (e.g. 0.001).

$$\log L(y_{1:T} | \theta) = -\frac{T}{2} \log(2\pi) - \frac{T}{2} \sum_{t=1}^T \left[\log |P_{yy,t|t-1}| + \frac{e_t e_t^T}{P_{yy,t|t-1}} \right] \quad (32)$$

where e_t and $P_{yy,t|t-1}$ are the innovations ($e_t = y_t - \hat{y}_t$) and innovation covariance matrix ($P_{yy,t|t-1} = S_{yy,t|t-1} S_{yy,t|t-1}^T$), respectively.

ALGORITHM II

SQUARE-ROOT CUBATURE RAUCH-TUNG-STRIEBEL SMOOTHER

• *Initialization:*

$$\hat{\mu}_{t|t} = \hat{\mu}_{t|T}, S_{t|t} = S_{t|T}$$

• *Time update:*

$$\mathcal{X}_{i,t|t} = S_{t|t} \xi_i + \hat{\mu}_{t|t}, \quad (33)$$

$$\mathcal{X}_{i,t+1|t}^* = \mathbf{F}(\mathcal{X}_{i,t|t}^x, \mathcal{X}_{i,t|t}^u, \mathcal{X}_{i,t|t}^\theta) \quad (34)$$

$$\hat{\mu}_{t+1|t} = \frac{1}{m} \sum_{i=1}^m \mathcal{X}_{i,t+1|t}^* \quad (35)$$

$$S_{t+1|t} = \text{qr}([X_{t+1|t}, \text{diag}(\sqrt{Q_T}, \sqrt{V_T}, \sqrt{W_T})]) \quad (36)$$

$$X_{t+1|t} = \frac{1}{\sqrt{m}} [\mathcal{X}_{1,t+1|t}^* - \hat{\mu}_{t+1|t}, \mathcal{X}_{2,t+1|t}^* - \hat{\mu}_{t+1|t}, \dots, \mathcal{X}_{m,t+1|t}^* - \hat{\mu}_{t+1|t}]. \quad (37)$$

$$P_{\mu',t+1|t} = X'_{t|t} X_{t+1|t}^T, \quad (38)$$

$$X'_{t|t} = \frac{1}{\sqrt{m}} [\mathcal{X}_{1,t|t} - \hat{\mu}_{t|t}, \mathcal{X}_{2,t|t} - \hat{\mu}_{t|t}, \dots, \mathcal{X}_{m,t|t} - \hat{\mu}_{t|t}] \quad (39)$$

$$A_t = (P_{\mu',t+1|t} / S_{t+1|t}^T) / S_{t+1|t}, \quad (40)$$

$$\hat{\mu}_{t|T}^S = \hat{\mu}_{t|t} + A_t (\hat{\mu}_{t+1|T}^S - \hat{\mu}_{t+1|t}), \quad (41)$$

$$S_{t|T}^S = \text{qr}([X'_{t|t} - A_t X_{t+1|t}, A_t S_{t+1|T}^S, A_t \text{diag}(\sqrt{Q_T}, \sqrt{V_T}, \sqrt{W_T})]) \quad (42)$$

III. SIMULATIONS

To demonstrate the performance of proposed deconvolution procedure, simulated fMRI data are used. We generate the simulated data by using hemodynamic model, which can be briefly described as: Neuronal activity u causes an increase in a vasodilatory signal s that is subject to auto-regulatory feedback. Blood flow f responds in proportion to this signal and causes change in blood volume v and deoxyhemoglobin content, q . The observed signal is nonlinear function of volume and deoxyhemoglobin. These dynamics are modeled by a set of differential equations (43) and an observation equation (44):

$$\begin{aligned} ds_t &= (\epsilon u - \kappa s_t - \vartheta(f_t - 1)) dt, \\ df_t &= s_t dt, \\ dv_t &= \tau(f_t - F(v_t)) dt, \\ dq_t &= \tau(fE(f_t) - F(v_t)q_t/v_t) dt, \end{aligned} \quad (43)$$

$$y_t = V_0 [k_1(1 - q_t) + k_2(1 - q_t/v_t) - k_3(1 - q_t)]. \quad (44)$$

Outflow is related to volume $F(v) = v^{1/\alpha}$ through Grubb's exponent α . The relative oxygen extraction $E(f) = \frac{1}{\varphi}(1 - (1 - \varphi)^{1/f})$ is a function of flow, where φ is a resting oxygen extraction fraction.

Our state vector is $\tilde{x}_t = [x_t, u_t, \theta_t]^T$, where $x_t = [s_t, f_t, v_t, q_t]$ and $\theta_t = \{\epsilon, \kappa, \vartheta, \tau, \alpha, \varphi\}$. The rest of the model parameters are constants. Here we consider two different simulation scenarios:

Simulation 1.: We generated a fMRI time course using the above hemodynamic model, where the input (neuronal activation) had a form of Gaussian function $u = \exp(\frac{1}{4}(t - 12)^2)$. We considered minor noise fluctuations for the input and hemodynamic states with variance $3 \cdot 10^{-3}$

and measurement noise with variance equals 1. The integration step was equal to the sampling interval ($\Delta t = 1$ s). The model inversion was then initialized with $x_0 = [0, 1, 1, 1]$; θ_0 within their physiological ranges (but different from values used for simulations); $v_0 = 0$; and error covariance matrices $\{P_0^{(x)} = I_{n_x} \cdot 10^{-2}, P_0^{(u)} = 1 \cdot 10^{-2}, P_0^{(\theta)} = I \cdot 10^{-4}\}$. All the noise components (covariances), except the input noise variance that we considered fixed $V = 0.1$, were adaptively approximated during SCKF step. Finally, we used integration step $\Delta t = 1/3$ s. In Fig. 1 we can see that the only forward estimation pass is not able to recover the true input signal, neither the hemodynamic states. However, the backward smoothing procedure already provides correct estimates.

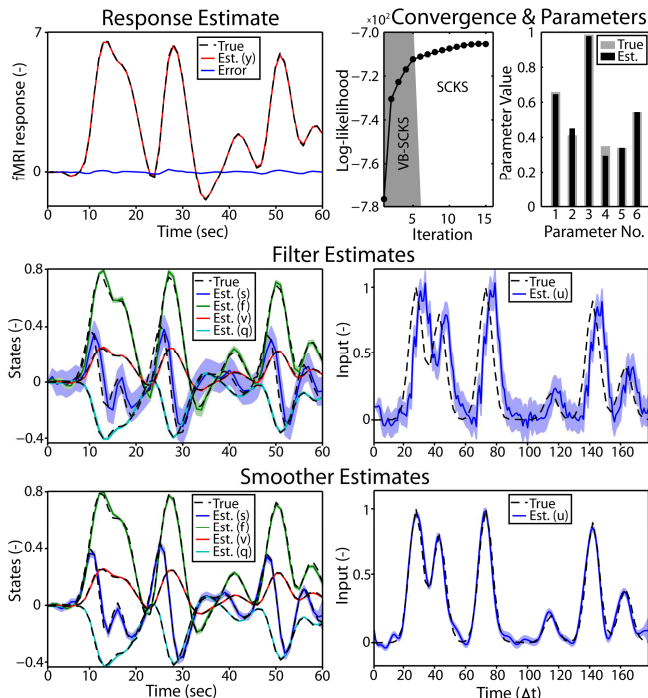


Fig. 1. Model inversion results for forward pass of SCKF and backward pass of SCKS, including estimates for hemodynamic states, input, parameters, and predicted hemodynamic response.

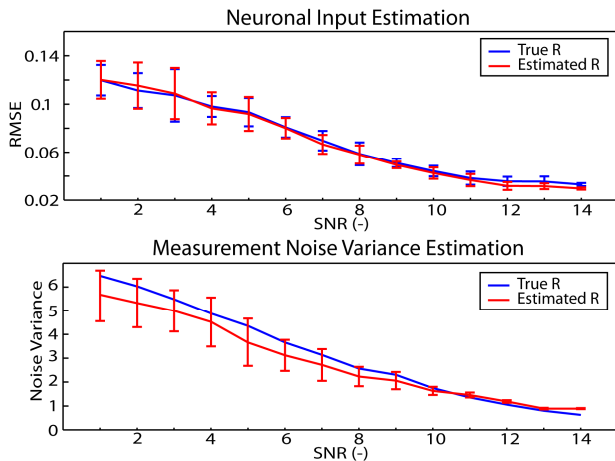


Fig. 2. Results of Monte Carlo simulations for the accuracy of neuronal input estimates (top) and estimates of measurement noise variance under different level of SNR.

Simulation 2: Next we performed Monte Carlo simulations for different amount of additive measurement noise with signal to noise ratio (SNR) from 1 to 14, where for each noise level we repeated generation and model inversion 50 times. The rest of fMRI time course generation and initialization was the same as in the Sim. 1. Finally, we compared performance of SCKS regarding an accuracy of the neuronal input estimate for scenarios when the measurement noise variance was assumed to be known and for the case it was adaptively estimated through VB approach (see Fig. 2). The inaccuracy between estimated and true neuronal input is expressed via root mean square error (RMSE).

IV. CONCLUSION

In this paper, we have introduced a robust blind deconvolution technique based on the nonlinear square-root cubature Kalman filter and Rauch-Tung-Striebel smoother, which allows an inference on hidden states, input, and model parameters. Critically, the measurement noise variance is adaptively estimated as well, through the efficient variational Bayesian approach. Proposed method is very general and can be applied to the inversion of any nonlinear continuous dynamic model that is formulated with stochastic differential equations. This description of the technique has focused on the estimation of neuronal synaptic activation by generalized deconvolution from observed fMRI data.

Finally it is evident that one can generalize this approach to dynamic causal modeling [10] and hope in improved identification of effective connectivity, with a possible application also to resting-state fMRI data.

REFERENCES

- [1] R. Buxton, E. Wong, and L. Frank, "Dynamics of blood flow and oxygenation changes during brain activation: the balloon model," *Magnetic Resonance in Medicine*, vol. 39, (no. 6), pp. 855-864, 1998.
- [2] K. Friston, A. Mechelli, R. Turner, and C. Price, "Nonlinear responses in fMRI: the Balloon model, Volterra kernels, and other hemodynamics," *NeuroImage*, vol. 12, pp. 466-477, 2000.
- [3] I. Arasaratnam and S. Haykin, "Cubature Kalman Filters," *IEEE Trans. Automatic Control*, vol. 54, pp. 1254-1269, 2009.
- [4] T. Ozaki, "A bridge between nonlinear time series models and nonlinear stochastic dynamical systems: a local linearization approach," *Statistica Sinica*, vol. 2, pp. 113-135, 1992.
- [5] J. Jimenez, "A simple algebraic expression to evaluate the local linearization schemes for stochastic differential equations* 1," *Applied Mathematics Letters*, vol. 15, pp. 775-780, 2002.
- [6] R. Van der Merwe, "Sigma-point Kalman filters for probabilistic inference in dynamic state-space models," Ph.D. thesis, University of Portland, Oregon, 2004.
- [7] M. Simandl and J. Dunik, "Design of derivative-free smoothers and predictors," *14th IFAC Symposium on System Identification*, Newcastle, Australia, pp. 1240-1245, 2006.
- [8] I. Arasaratnam and S. Haykin, "Nonlinear Bayesian Filters for Training Recurrent Neural Networks," *MICAI 2008: Advances in Artificial Intelligence*, pp. 12-33, 2008.
- [9] S. Sarkka and A. Nummenmaa, "Extension of VB-AKF to estimation of full covariance and nonlinear systems." *IEEE Trans. Automatic Control*, 2011, In Press.
- [10] K. J. Friston, L. Harrison, W. Penny, "Dynamic causal modelling." *Neuroimage*, vol. 19, pp. 1273-1302, 2003.